Smart Structures and Systems, Vol. 4, No. 1 (2008) 35-46
DOI: http://dx.doi.org/10.12989/sss.2008.4.1.035

Comparisons of smart damping treatments based on FEM modeling of electromechanical impedance

C. P. Providakis†

Department of Applied Sciences, Technical University of Crete, Chania, Greece

D.-P. N. Kontoni

Department of Civil Engineering, Technological Educational Institute of Patras, Patras, Greece

M. E. Voutetaki and M. E. Stavroulaki

Department of Applied Sciences, Technical University of Crete, Chania, Greece

(Received January 26, 2005, Accepted March 6, 2007)

Abstract. In this paper the authors address the problem of comparing two different smart damping techniques using the numerical modelling of the electro-mechanical impedance for plate structures partially treated with active constrained layer damping treatments. The paper summarizes the modelling procedures including a finite element formulation capable of accounting for the observed behaviour. The example used is a smart cantilever plate structure containing a viscoelastic material (VEM) layer sandwiched between a piezoelectric constrained layer and the host vibrating plate. Comparisons are made between active constrained layer and active damping only and based on the resonance frequency amplitudes of the electrical admittance numerically evaluated at the surface of the piezoelectric model of the vibrating structure.

Keywords: smart damping; ACDL; electomechanical impedance; FEM; piezoelectric actuators/sensors.

1. Introduction

There has been an extensive use of passive and active surface treatment strategies for damping the vibration of structures since the 80s. Important among these strategies is the active constrained layer damping (ACLD) treatment (Shen 1994, Baz 1997, Hau and Fung 2004, Liu, *et al*. 2004). A typical ACLD consists of a VEM layer sandwiched between the host structure and the active constrained layer, which is made of smart materials such as piezoelectric ceramics rather than conventional materials. The active layer can function as a conventional constraining layer to increase the energy dissipation by enhancing the shear strain in the damping layer. It is now well established that the active constrained layer damping configuration (ACLD) can be designed and is more effective to reduce the lower frequency modes. The idea of combining active materials such as piezoelectric materials, with viscoelastic

†Corresponding Author, E-mail: cpprov@mred.tuc.gr

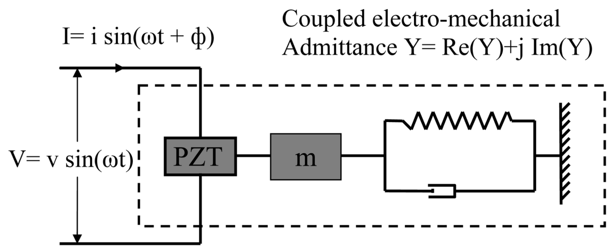

Fig. 1 A schematic description of a PZT actuated dynamic system

materials (VEM) to produce an active constrained layer has been also attractive since the added passive damping provides a fail-safe mechanism and improves the stability and robustness of the system. On the other hand, it is well known that VEM reduces the transmissibility of the control force of the active layer and therefore, several different types, of ACLD treatments should be investigated in detail to perform more effective controllability and in the same time more vibration reduction when compared to purely active damping systems. Further, the modeling and analysis of active constrained layer damping (ACLD) system represent a high level of sophistication and complexity from the structural analysis viewpoint.

The finite element method has become a powerful and versatile tool in designing smart structures containing piezoelectric sensors and actuators. Numerous theories and modeling techniques relating to the finite element method have been proposed for the analysis of adaptive piezoelectric structures (Van Nostran 1994, Varadan, *et al*. 1996, Lim, *et al*. 1999, Kim, *et al*. 1996, Wang, *et al*. 2004, Littlefield, *et al*. 2002).

Any active material system with integrated induced strain actuators can be generalized as a 1-D simple-electromechanical system as shown in Fig. 1. The entire electro-mechanical system may be electrically represented by electrical impedance which is affected by the dynamic characteristics of the host vibrating structure. In other words, the electromechanical admittance (inverse of electrical impedance) is modified by structural damping and/or stiffness. Any change in the electrical impedance (admittance) signature is considered as an indication of a change in structural damping and/or stiffness. Therefore, the electromechanical impedance (EMI) of the electrical model describes very accurately the dynamic behaviour of the smart structural systems.

The purpose of the present work is to provide a numerical technique for the comparison of different damping treatments for suppressing the vibrations of smart structures. It focuses on comparing the effect of active constrained layer damping (ACLD) treatments with purely active damping (AD) treatments on the system damping of a smart plate. A cantilever plate with partial damping treatment is modelled by using the finite element method. Finally simulation results are presented for the damping reduction of the first few modes of vibration.

2. Fem modelling and formulation

In this paper, it is assumed that layers are perfectly bonded together. Also the finite element formulation adopted here is restricted to linear elastic material behaviour, small strain and displacements. The linear constitutive equations for piezoelectric materials expressing the coupling between the elastic and the electric field can be expressed as:

$$\sigma = C\varepsilon + hE$$
$$D_e = h^T E + bE \tag{1}$$

Where σ is the stress vector, C is the stiffness matrix, ε is the strain vector, h is the matrix of piezoelectric constants, E is the electric field, D_e is the electric displacement and b is the permittivity matrix. The strain-displacement equations can be drawn as:

$$\varepsilon_{ij} = \frac{1}{2}(\bar{u}_{i,j} + \bar{u}_{j,i}) \tag{2}$$

where $\bar{u}$ and comma denote differentiation with respect to the coordinates. The electric field E can be expressed in terms of the electric potential as:

$$E = -\nabla\phi \tag{3}$$

where ϕ is the electric potential

The generalized coordinates are related to the displacements and the electric potential as:

$$\bar{u} = N_u u$$
$$\bar{\phi} = N_\phi \phi \tag{4}$$

where N_u and N_ϕ are the matrices of the shape functions for the displacement and potential, respectively. Thus, the strains can be written in terms of the displacements at nodes by the expression:

$$\varepsilon = B_u u \tag{5}$$

where B_u is the product of the differential operating matrix of the strain – displacement equation and the shape function matrix N_u, respectively.

Putting the electric field-potential relation in terms of the nodal potential yields

$$E = -\nabla N_\phi \Phi = -B_\phi \Phi \tag{6}$$

The finite element formulation for dynamic analysis of piezoelectric material can be derived from the principle of minimum potential energy by means of a variational functional. This formulation has been presented in many papers (e.g. Tzou and Tseng 1990, Rao and Sunar 1993) and can be described in written partition form as:

$$[M_{uu}]\ddot{u} + [K_{uu}]u + [K_u]\Phi = \{F\}$$
$$[K_{u\phi}^T]u + [K_{\phi\phi}]\Phi = \{Q\} \tag{7}$$

where $[M_{uu}] = \int p N_u^T N_u dV$, kinematically constant matrix

$[K_{uu}] = \int B_u^T C^E B_u dV$, elastic stiffness matrix

$[K_{u\phi}] = \int B_u^T h^T B_\phi dV$, piezoelectric coupling matrix

$[K_{\phi\phi}] = -\int B_{\phi}^{T} b^{S} B_{\phi} dV$, dielectric stiffness matrix

$\{F\} = \int_{A_1} N_{A_1} f_S dA_1 + \int_V N_b^T f_b dV + N_a^T f_c$, mechanical force

$\{Q\} = -\int_V N_{A_2}^T q_S dA_2 - N_S^T q_c$, electrical charge

where f_b, is the body force, f_s, is the surface force, f_c, is the concentrated force, q_s is the surface charge, q_c is the point charge, A_1 is the area where mechanical forces are applied and A_2 is the area where electrical charges are applied.

If the time harmonic case is considered here the displacements and electrical potential are given by the expressions:

$$\begin{aligned} \{u(t)\} &= \{u\}e^{i\omega t} \\ \{\Phi(t)\} &= \{\Phi\}e^{i\omega t} \end{aligned} \tag{8}$$

where $i = \sqrt{-1}$ and ω is the undamped, angular frequency.

Consequently, the forces and charges can be expressed as:

$$\begin{aligned} \{F(t)\} &= \{F\}e^{i\omega t} \\ \{Q(t)\} &= \{Q\}e^{i\omega t} \end{aligned} \tag{9}$$

Combining the above equations with (7) we can obtain the followings equation:

$$\left(-\omega^2\begin{bmatrix} [M_{uu}] & 0 \\ 0 & 0 \end{bmatrix} + \begin{bmatrix} [K_{uu}] & [K_{u\phi}] \\ [K_{u\phi}] & [K_{\phi\phi}] \end{bmatrix}\right)\begin{Bmatrix} \{u\} \\ \{\Phi\} \end{Bmatrix} = \begin{Bmatrix} \{F\} \\ \{Q\} \end{Bmatrix} \tag{10}$$

The response then can be obtained in the frequency domain for the displacements $\{u\}$ and potential $\{\Phi\}$, for a given charge of force excitation at a given angular frequency. It should be noted that all these vectors must now be considered as complex amplitudes.

Constrained active layer damping consists of three layers: the host plate, the viscoelastic layer and the piezoelectric constraining layer. The viscoelastic layer, being much softer than the host plate and constrained layer, has considerable transverse shear deformations. In order to model this difference, the viscoelastic layer needs to deform differently from the structure or the constrained layer. In this paper, in order to account for the different deformation of each layer the viscoelastic, the host structure and the constraining layer are modelled separately with different finite elements.

The idea of moving a piezoelectric actuator from direct contact with the host structure and placing a viscoelastic layer between the host structure and the piezoelectric actuator is questionable. The actuator is more effective in applying force when it is acting directly at the host structure rather than through a very soft damping material as being the viscoelastic one. However an active constraining layer can significally enhance the damping effectiveness via active control. In comparing different types of damping treatments, the active constrained layer (ACLD) and the pure active layer (AD) using piezoelectric film actuators are designed along with the host structure in this paper to demonstrate the potential of each type of treatments (Fig. 2). In order to perform the comparison studies of different damping configurations,

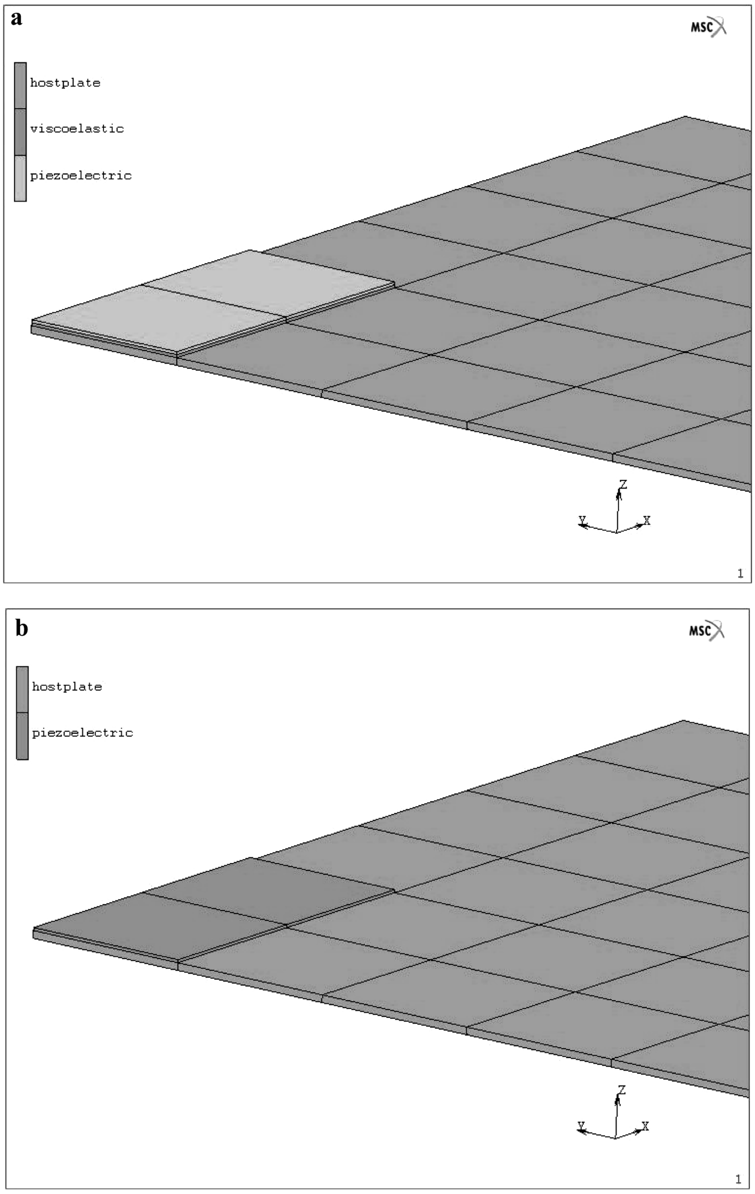

Fig. 2 a) ACLD treatment; b) AD treatment

coupled electro-mechanical harmonic analyses are performed by using the finite element program MSC. MARC2005 (MSC 2005) enhanced by its piezoelectric analysis capabilities.

3. The electromechanical impedance feature

During the last few years the Electro-Mechanical Impedance (EMI) technique has demonstrated its potential for cost-effective structural monitoring for a wide range of engineering structures (Ayres, *et al.*

1998, Bhalla, *et al.* 2005, Littlefield, *et al.* 2002, Soh, *et al.* 2000, Tseng and Wang 2005). The key point of the impedance-based qualitative monitoring technique is the electromechanical coupling of the piezoelectric PZT actuator/sensor patch. The PZT patches are made of piezoelectric materials, which generate surface charges in response to applied mechanical stresses and conversely undergo mechanical deformation in response to applied electric fields. Hence, when a PZT patch surface of length l_p, width w_p, and thickness h_p bonded to the monitored structure is electrically excited by means of a harmonic voltage $V = V_o \gamma e^{j\omega t}$, in the direction of its thickness it produces deformations in the surrounded local area of the host structure. The response of this area is transferred back to the PZT patch in the form of admittance function (admittance is the reciprocal of impedance), comprising the conductance (the real part) and the susceptance (the imaginary part).

The acquisition of the coupled electromechanical impedance can be performed by providing a constant voltage (1 V) to the PZT patch over a pre-set frequency range. The magnitude and phase of the steady state current draw (after transient decay) of the PZT is recorded in real and imaginary admittance. The variation in the electrical admittance over the pre-selected frequency is due to two factors: (1) the electrically capacitive nature of the PZT, and (2) the interaction between the PZT and the structure to which it is bounded. The variations in the capacitive nature show up as a gradual change in the impedance curve, whereas the structural interaction corresponds to sharp peaks that represent part of structural resonance. Therefore, any change in the dynamic behavior of the host structure like the damping characteristics will result in an electrical admittance change.

Following the above description when a unit voltage is applied to the piezoelectric layer of the finite element model of the active constrained damping layer the admittance could be calculated. The application of the unit voltage is simulated by considering a positive and a negative electrode located at the upper and lower, respectively, surface of the PZT patch. In the model these electrodes are made by tying the potential degree of freedom of all the nodes belonging to an electrode to one node. In this way the electric current passing through the PZT patch can be given by the following equation:

$$I = (i\omega) \int_{-l_p/2}^{l_p/2} \int_{-W_p/2}^{W_p/2} D\,dx\,dy \tag{11}$$

which, in turn, by applying Gauss law can be expressed in terms of total charge on the electrode surface as:

$$I = i\omega \sum Q_i \tag{12}$$

The admittance is the ratio of the resulting current and the applied voltage. Thus, the resulting admittance Y is related to the total reaction charge on the piezoelectric surface as:

$$\bar{Y} = i\omega - \sum_{l} Q_i \tag{13}$$

Where ΣQ_i is the sum of the reaction charges resulted from the finite element analysis on all nodes belonging to the appropriate piezoelectric electrode. The finite element program automatically performs this summation since all the nodes of an electrode are tied to one node. Since a unit voltage is applied to the PZT patch, conductance can be computed as the real part of the resulted admittance and suscuptance as the imaginary part. These electrical “signatures” of the structure (in the frequency domain), contain vital information concerning the phenomenological nature of the structural parameters i.e., the stiffness, the damping and the mass. The structural dynamic behavior corresponds to a unique pattern of the sharp peaks generated above the baseline electrical capacitive admittance in the admittance – frequency plots.

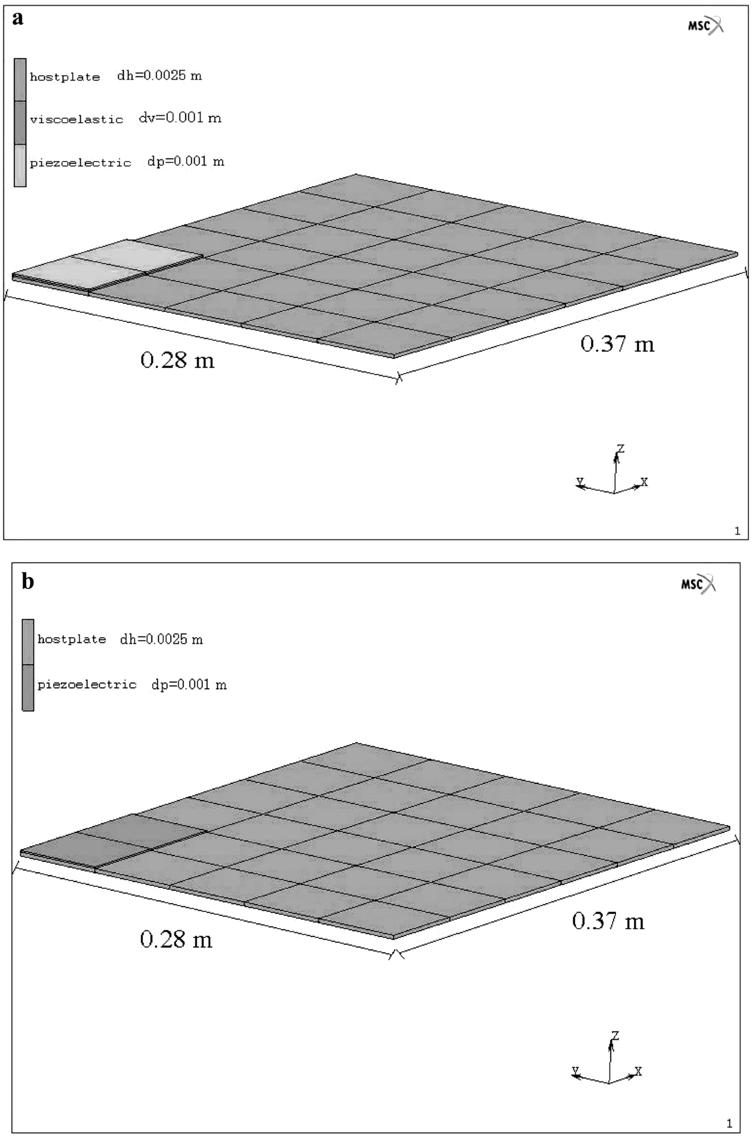

Fig. 3 a) ACLD finite element model; b) AD finite element model

4. Numerical example

The purpose of this section is to numerically evaluate and to compare the damping resulting from an active constrained damping layer (ACLD) system and a purely active damping system (AD). A thin aluminum cantilever plate, which is partially treated with a viscoelastic (VEM) material which also has attached to its surface a piezoelectric actuator, is studied. The VEM layer is under the actuator for the ACLD as can be seen in Fig. 2 and considered as perfectly bonded to each other. This is a relative simple structure and it is assumed that there is no structural damping so as to show clearly the effects of active restrained and purely active damping. It is also assumed that the piezoelectric elements are

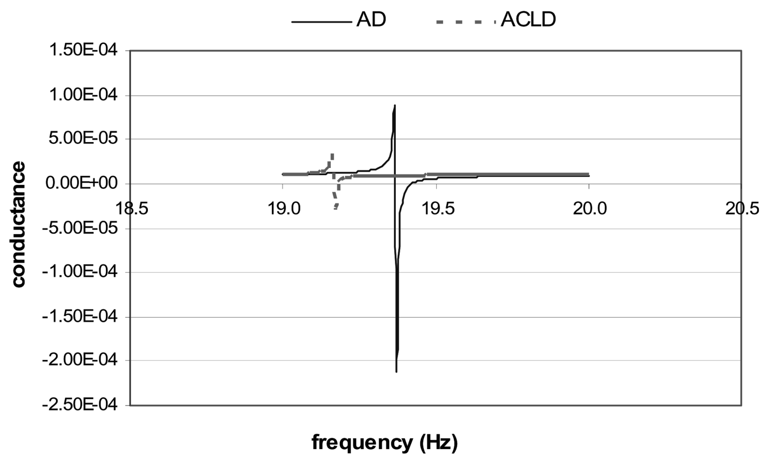

Fig. 4 Conductance signature for the 1st mode of ACLD, AD cases

bonded perfectly to the host plate and to the VEM for the case of purely active (AD) and active constrained layer damping (ACLD) model, respectively. The nodes at the interface of the PZT and VEM (for the ACLD case) and at the interface of the PZT and host plate (for the AD case), respectively, are connected to the common ground to make a closed circuit for the potential. In both ACLD and AD plate cases there is not control loop that regulates the piezoelectric actuator and the structure response. Two 8-node piezoelectric solid elements (Fig. 3) are used to model the PZT devices each of which have four degrees of freedom, the first three are for the *x*-, *y*-, and *z*- displacements, and the fourth is for the electric potential. The material parameters for the PZT devices are ρ_a = 7500 Kgr/m^3, $E_a = 3.6\times10^{11}$N/m^2 and $\nu_a = 0.3$.

To model the VEM layer, two 8-node solid finite elements (Fig. 3) are assumed with a viscoelastic relax function for the shear modulus given by $G(t) = 100+9900e^{(t/0.4170316)}$, while $E_v = 2\times10^7$ N/m^2 and $\nu_v = 0.3$. The host aluminum plate is modeled by 8-node solid elements (Fig. 3) with boundary conditions: one short side of the host plate is clamped and the others are free. The material properties of the host plate are ρ_p = 2700 Kgr/m^3, $E_p = 9\times10^{10}$ N/m^2 and $\nu_p = 0.3$. The dimensions of the host plate

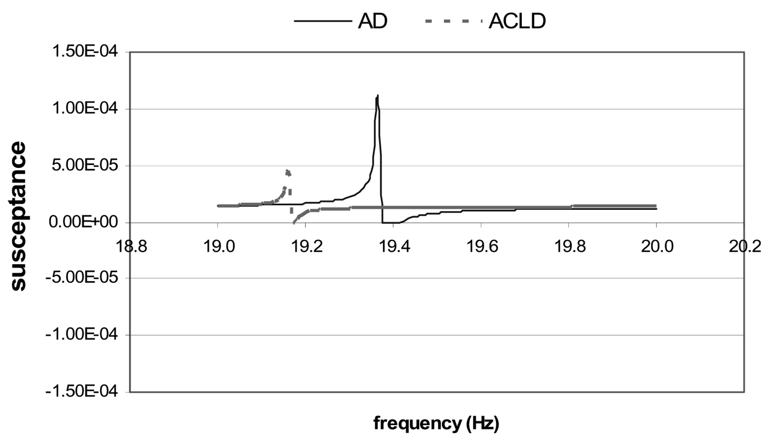

Fig. 5 Susceptance signature for the 1st mode of ACLD, AD cases

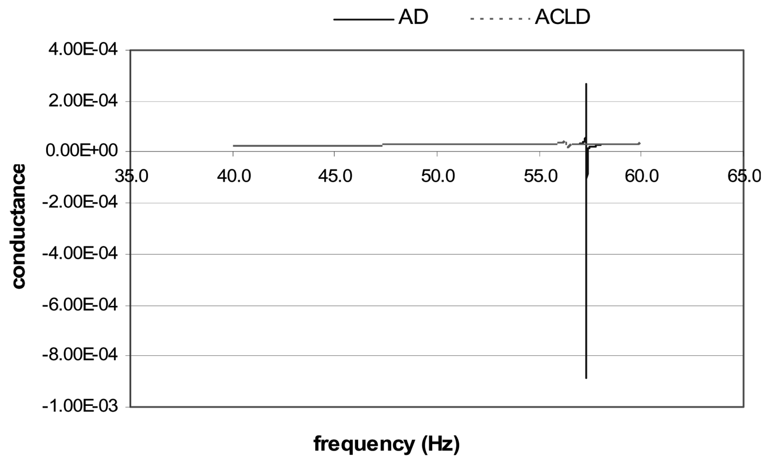

Fig. 6 Conductance signature for the 2^{nd} mode of ACLD, AD cases

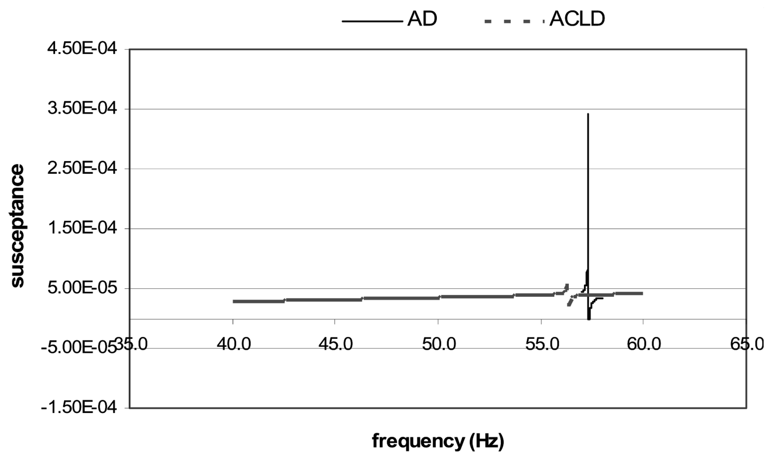

Fig. 7 Susceptance signature for the 2^{nd} mode of ACLD, AD cases

are 0.35 m × 0.28 m while the thickness of piezoelectric, viscoelastic and host plate layer are 0.001 m, 0.001 m and 0.0025 m, respectively.

Fig. 4 and 5 depict the frequency response of the conductance and susceptance, respectively, amplitudes as resulted on the electrical surfaces of the piezoelectric patch model. The solid line represents the frequency response of the AD treatment while the dashed line represents the ACLD treatment. It is evident that activating the ACLD treatment has resulted in effective attenuation of both conductance and susceptance amplitudes. Also, it is evident that the use of ACLD treatment has resulted in shifting the frequency of the ACLD treatment to lower first resonance mode frequencies than that of AD treatment.

Comparisons are also shown in Fig. 6 and 7 between amplitudes of frequency responses of conductance and susceptance, respectively, when ACLD and AD treatment are activated for frequencies closed to their second resonance mode. It can be seen that the added damping obtained by applying an active constrained layer reduces the response of both conductance and susceptance considerably. In this second resonance mode the shift of the resonance frequency is lower than that observed in the first resonance mode.

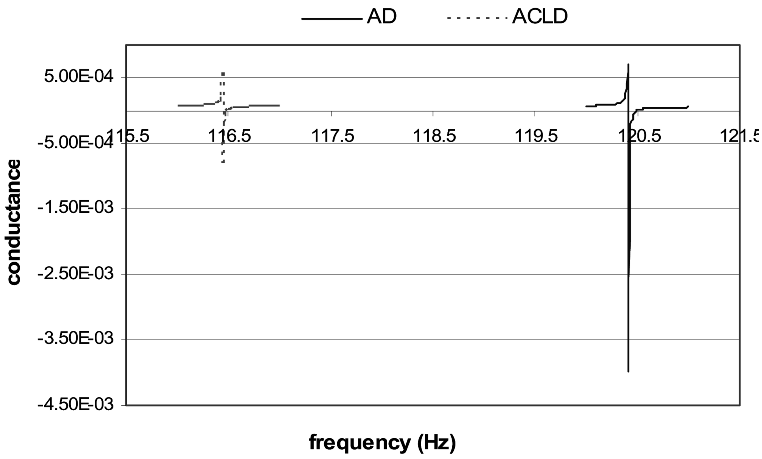

Fig. 8 Conductance signature for the 3rd mode of ACLD, AD cases

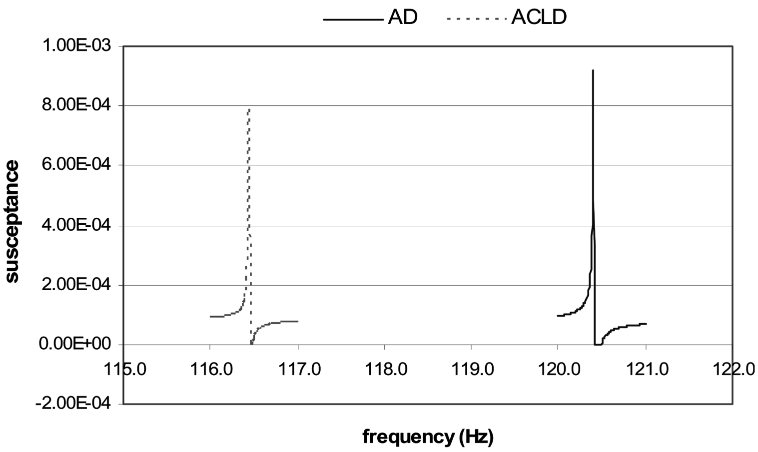

Fig. 9 Susceptance signature for the 3rd mode of ACLD, AD cases

The same, as above, results are displayed, clearly, in Figs. 7 and 8 where it is summarized that the ACLD treatment strategy is very effective in attenuating the frequency response of conductance and susceptance at their third resonance mode. However, this attenuation is much lower that that obtained with the ACLD treatment at the first two resonance modes. Hence, it is conducted that the ACLD treatment is superior to the AD treatment particularly over wide frequency ranges. Such superiority stems from its ability to combine the attractive attributes of both passive and active controls to produce lower amplitude responses of both conductance and susceptance values.

5. Conclusions

The present paper has presented a numerical finite element comparison study of vibrating plates, which are partially treated with smart damping treatments, based on the electromechanical impedance approach.

Comparison studies have been presented which examine the performance of the active constrained damping layer (ACLD) model relative to the purely active (AD) model. These studies enabled a complete description of the numerical evaluation of the electrical input admittance of the damping systems and a faithful reproduction of the dynamical characteristics of the systems.

The ability of the ACLD treatments to attenuate both the electromechanical conductance and susceptance values has been successfully demonstrated.

Hence, the electromechanical impedance approach, used in the present work, constitutes an invaluable tool for predicting the performance of smart damping treatments that could be used in many engineering applications.

Acknowledgements

The authors acknowledge financial support by “Archimedes - EPEAEK II Research Programme” co-funded by European Social Fund and National Resources.

References

Ayres, J. W., Lalande, F., Chandhvy, Z. and Rogers L. A. (1998), “Qualitative impedance-based health monitorind of civil infrastructures”, *Smart Mater. Struct.*, **7**, 599-605.

Baz, A. (1997), “Boundary control of beams using active constrained layer damping”, *J. Vib. Acoustics*, **119**, 116-172.

Bhalla, S., Soh, C. K. and Liu, Z. (2005), “Wave propagation approach for NDE using surface bonded piezoceramics”, *NDT & E Intrn.*, **38**, 143-150.

Hau, L. C. and Fung, E. H. K. (2004), “Effect of ACLD treatment confifuration on damping performance of a flexible beam”, *J. Sound Vib.*, **269**, 549-567.

Kim, J., Varadan, V. V. and Varadan, V. K. (1996), “Finite element modeling of a smart cantilever plate and comparison with experiments”, *Smart Mater. Struct.*, **5**, 165-170.

Lim, Y. H., Varadan, V. V. and Varadan, V. K. (1999), “Closed loop finite element modeling of active structural damping in the time domain”, *Smart Mater. Struct.*, **8**, 390-400, 1999.

Littlefield, A., Fair-Weather, J. and Craig, K. (2002), “Use of FEA derived impedances to design active structures”, *J. Intelligent Material System and Structures*, **13**, 377-388.

Liu, T., Hua, H. and Z. Zhang, Z. (2004), “Robust control of plate vibration via active constrained layer damping”, *Thin-Walled Structures*, **42**, 427-448.

MSC. MARC 2005, Users Guide, MSC. Software, CA, USA, 2005

Rao, S. S. and Sunar, M. (1993), “Analysis of distributed thermopiezoelectric sensors and actuators in advanced intelligent structures”, *AIAA J.*, **131**, 1280-1286.

Shen, I. Y. (1994), “Hybrid damping through intelligent constrained layer damping treatments”, *ASME J. Vib. Acoust.*, **116**, 341-349.

Soh, C. K., Tseng, K. K. H., Bhalla, S. and Gupta, A. (2000), “Performance of smart piezoceramic patches in helth monitoring of a RC Bridge”, *Smart Mater. Struct.*, **9**, 533-542.

Sun, F. P., Chaudhvy, Z. Rogers, C. A., Majmn, M. and Liang, C. (1995), “Automatel real-time structure health monitoring via signature pattern recognition”, *Proceedings of SPIE conference on Smart Structures and Materials*, San Diego, CA. **7**, 559-605.

Tseng, K. K. and Wang, L. (2005), “Structural damage identification for thin plates using smart piezoelectric transducers”, *Comp. Meth. Appl. Mech. Eng.*, **194**, 3192-3209.

Tzou, H. S. and Tseng, C. I. (1990), “Distributed piezoelectric sensor/actuator design for dynamic measurement control of distributed parameter systems : a piezoelectric finite element approach”, *J Sound Vib.*, **138**, 17-34.

Van Nostran, W. C., Knowles, G. and Iuman, D. (1994), "Finite element model for active constrained damping", *Proc. Conf. Smart Struct. Mater. SPIE*, **2173**, 269-281.

Varadan, V. V., Lim, Y. and Varadan, V. K. (1996), "Closed loop finite element modeling of active/passive damping in structural vibration control", *Smart Mater. Struct.*, **5**, 685-694.

Wang, Q., Duan, W. H. and Quek, S. T. (2004), "Repair of notched beam under dynamic load using piezoelectric patch", *Int. J. Mech. Sci.*, **46**, 1517-1533.

CC